**Student Seminar – HASCO 2014**
**Göttingen, 1.08.2014**

# Measurements of normalized differential cross-sections for *ttbar* production in *pp* collisions at s = 7 TeV using the ATLAS detector


**Speakers**

**Gioan Tatsi** *University of Strathclyde*

**Valeria Botta** *University of Pisa*

**Tutor**

**Mark Owen** *Manchester University*

# Outline

- Top Quark features
- Why are we interested?
- Where to look?
- How was it measured?
- Key Definitions
- Object Id and Reconstruction
- Event Selection
- Unfolding
- Uncertainties
- Results
- Comparison beteween Data and Predictions

# Top quark

- The top quark is the most massive among the elementary particles with a **mass** of about 173 GeV.
- It has a **lifetime** of about $5 \cdot 10^{-25}$ s.
- This is about 20 times shorter than the time-scale of strong interactions, therefore it decays before forming hadrons.

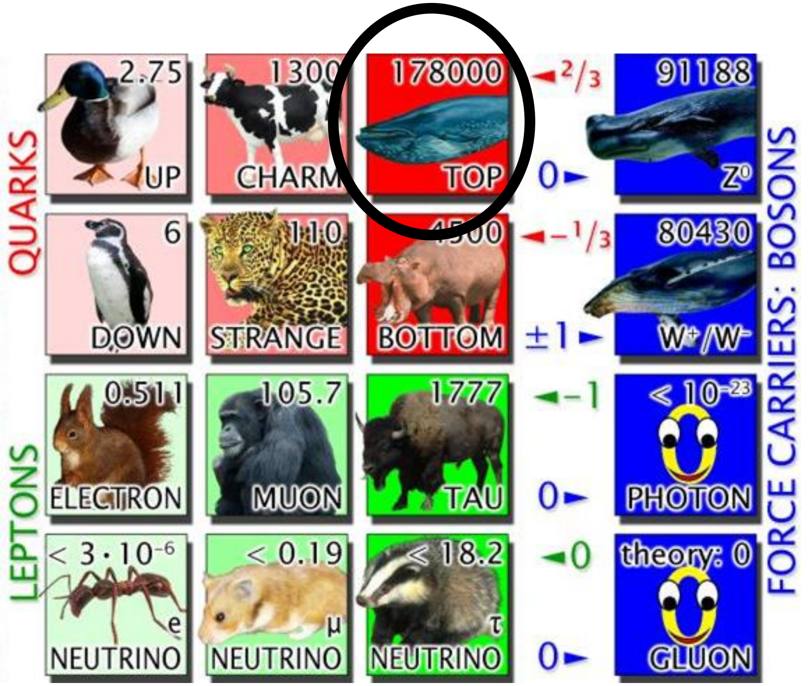

# Why are we interested ?

1) Unique opportunity to study a “bare” quark
2) The top quark plays an important role in many theories beyond the Standard Model (SM)
3) Differential measurements have been proposed to be sensitive to new-physics effects
4) Large number of events at the LHC → precise differential cross-section measurements → precision test based on perturbative QCD

# Where to look ?

- In the SM, the top quark decays almost exclusively into a W boson and a b-quark. Thus we look in the W boson decay modes.
- This analysis makes use of the lepton+jets decay mode, good compromise between statistics and signal purity.
- The lepton is either an electron or a muon. In this paper, muons and electrons from tau decays are not discarded.

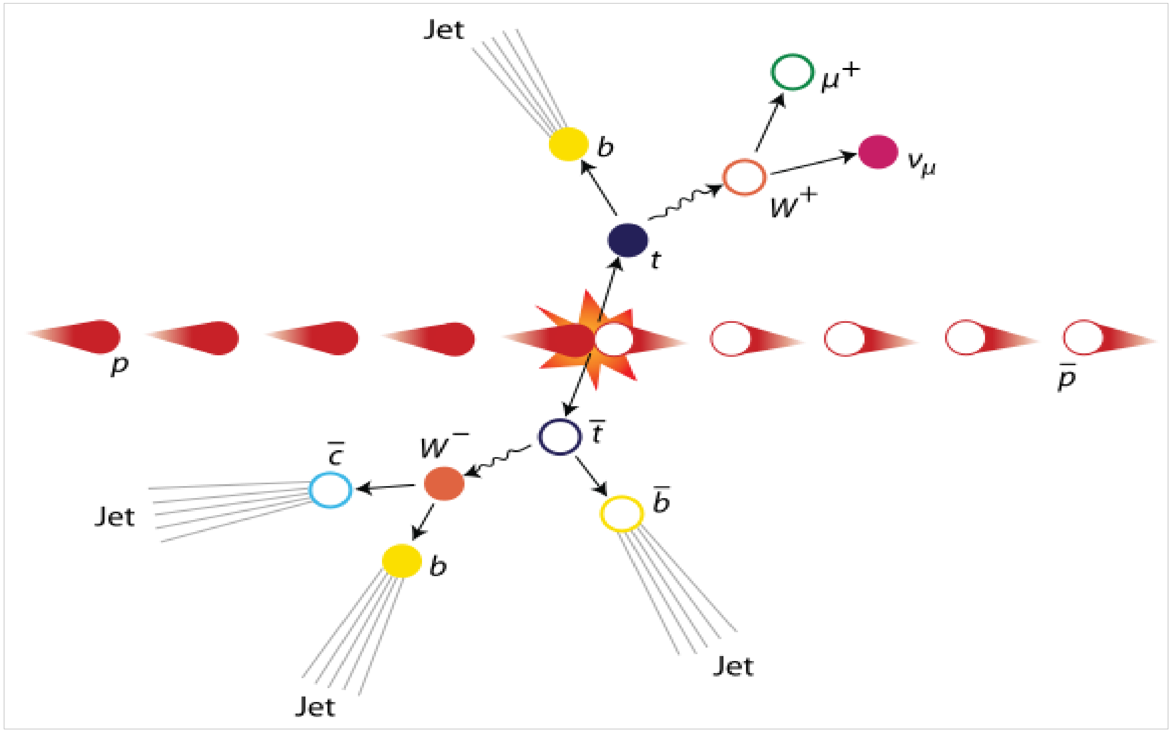

# How was it measured ?

- Using  the ATLAS detector at the LHC
- Dataset: proton proton collisions at a center-of-mass energy of 7 TeV in 2011, corresponding to an integrated luminosity of  4.6 $fb^{-1}$

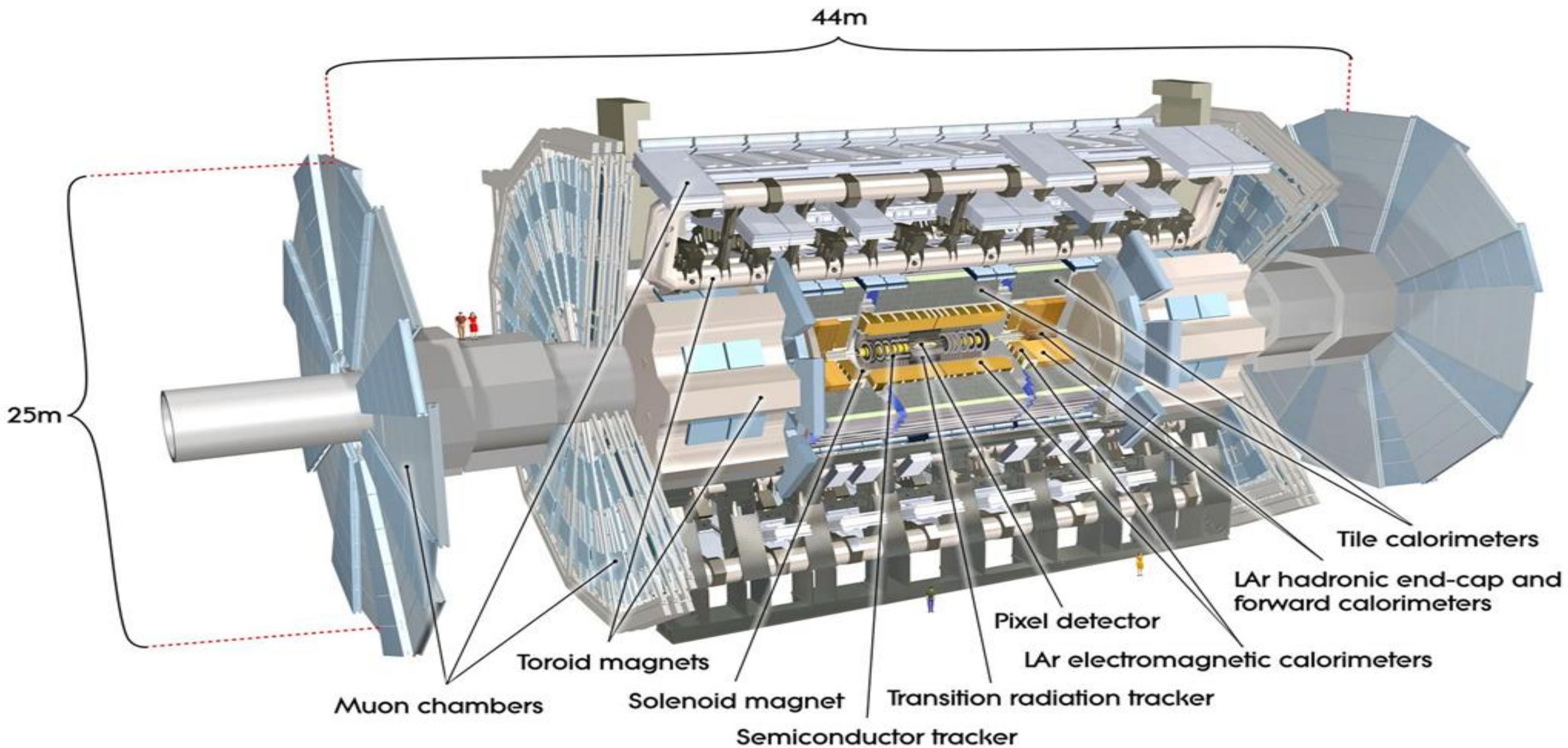

# Key Definitions

- **Cross-section σ** : expresses the likelihood of interaction between particles.
- **Branching Ratio (BR) :** is the ratio of particles which decay by an individual decay mode with respect to the total number of particles which decay.
- **Differential cross-section**:

$$\frac{d\sigma}{dX_j} \equiv \frac{1}{\Delta X_j} \cdot \frac{\sum_i \mathcal{M}_{ji}^{-1}[D_i - B_i]}{\text{BR} \cdot \mathcal{L} \cdot \epsilon_j},$$

where $X_j$ is the bin width, $D_i$ ($B_i$) are the data (expected background) yields in each bin i of the reconstructed variable, $\mathcal{L}$ is the integrated luminosity of the data sample, $\varepsilon_j$ is the event selection efficiency, and BR = 0.438 is the branching ratio of $t\bar{t} \to \ell$+jets. The matrix element $\mathcal{M}^{-1}_{ji}$ performs the unfolding procedure.

# Object Reconstruction and Identification

- The **primary vertex** is chosen to be the vertex with the highest $\Sigma p_T^2$ over all associated tracks with $p_T > 0.4$ GeV.
- Strict quality requirements are applied to the shape of the energy deposition in the EM calorimeters and to the **electron** track variables: $E_T > 25$GeV and $|\eta\_cluster| < 2.47$.
- **Muon** candidates are reconstructed by combining track segments in different layers of the muon chambers. Requirements for muons are $p_T > 25$ GeV and $|\eta| < 2.5$.
- Electron and muon candidates are required to be **isolated** in order to reduce the background from hadrons mimicking lepton signatures and leptons from heavy flavor decays.
- **Jets** are reconstructed from topological clusters of energy depositions using the anti-kt algorithm with a radius parameter of R= 0.4.
- The **missing transverse momentum** vector $E_T^{miss}$ is derived from the vector sum of calorimeter cell energies within $|\eta| < 4.9$
- The identification of ttbar events is improved by tagging jets originating from b-quarks using a combination of three **b-tagging** algorithms.

# Event Selection

| Event selection | |
|---|---|
| Trigger | Single lepton |
| Primary vertex | $\geq 5$ tracks with $p_{\mathrm{T}} > 0.4\,\mathrm{GeV}$ |
| Exactly one | Muons: $p_{\mathrm{T}} > 25\,\mathrm{GeV}$, $\lvert\eta\rvert < 2.5$ |
| isolated lepton | Electrons: $p_{\mathrm{T}} > 25\,\mathrm{GeV}$ |
| | $\lvert\eta\rvert < 2.47$, excluding $1.37 < \lvert\eta\rvert < 1.52$ |
| $\geq 4$ jets | $p_{\mathrm{T}} > 25\,\mathrm{GeV}$, $\lvert\eta\rvert < 2.5$ |
| $b$-tagging | $\geq 1$ $b$-tagged jet at $\epsilon_b = 70\%$ |
| $E_{\mathrm{T}}^{\mathrm{miss}}$ | $E_{\mathrm{T}}^{\mathrm{miss}} > 30\,\mathrm{GeV}$ |
| $m_{\mathrm{T}}^{W}$ | $m_{\mathrm{T}}^{W} > 35\,\mathrm{GeV}$ |
| Kinematic fit | $\log(\mathscr{L}) > -50$ |

# Kinematic Reconstruction

- It's necessary to reconstruct the whole event kinematics, that is assigning jets to the hard process particles. It is done through testing all possible permutations and choosing the assignment that gives a maximum likelihood value.

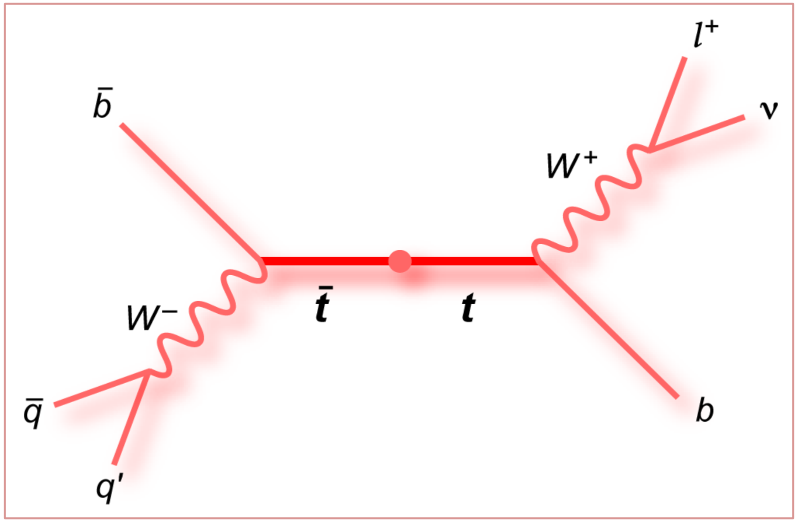


- Kinematic costraints given by the known invariant masses are applied.
- In order to separate properly from poorly reconstructed events, it is required that the event satisfy the condition: $\log(\mathcal{L}) > -50$.

# Unfolding

- A particle with a given $p_T$ value can be reconstructed with another $p_T$ value, therefore changing the **differential distribution** (same for all the other variables).
- This effect can be evaluated only on **simulated samples** and then used to correct the data.

- Example: $p_T$ of the hadronically decaying top at parton and reco level.

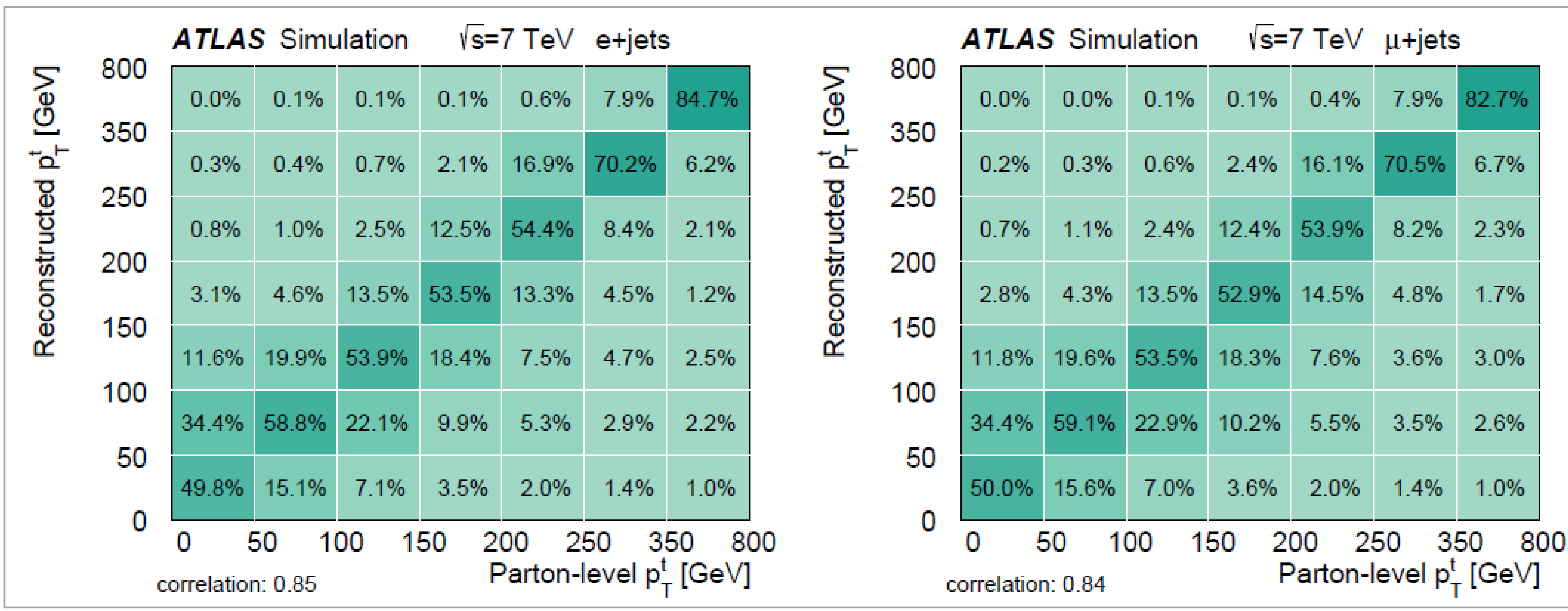

# Uncertainties

❖ Uncertainty is dominated by **systematics**

- **detector** modeling (JES, resolution,…)
- **signal** modeling (choice of MC generator, PDFs, ..)
- **background** modeling

❖ The uncertainty is evaluated for each source by varying the nominal value by one standard deviation upwards and downwards and then propagating the effect through the whole analysis.

❖ Most important **contributions**

- for top $p_T$ and m(ttbar)
  - JES
  - signal generator,
  - b-tagging efficiency
- for ttbar $p_T$
  - IFSR
- for ttbar y
  - signal generator
  - fragmentation

# Results

## Unfolded and combined results

### INCLUSIVE CROSS SECTION
combined e+μ channels

**σ =160 pb** with 15% uncertainty, in agreement with the SM prediction.

### DIFFERENTIAL CROSS SECTION

✓ In fair **agreement** with predictions

➢ some **discrepancy** on top $p_T$

➢ **dependance** on mc generator and parton shower modeling and on PDFs choice for different kinematc variables

| $p_T^t$ [GeV] | $\frac{1}{\sigma}\frac{d\sigma}{dp_T^t}$ $[10^{-3}\mathrm{GeV}^{-1}]$ | Stat. [%] | Syst. [%] |
|---|---|---|---|
| 0 – 50 | 3.4±0.2 | ± 2.6 | ± 5.1 |
| 50 – 100 | 6.7±0.1 | ± 1.0 | ± 1.9 |
| 100 – 150 | 5.3±0.2 | ± 1.6 | ± 2.6 |
| 150 – 200 | 2.6±0.1 | ± 1.9 | ± 4.8 |
| 200 – 250 | 1.12±0.06 | ± 2.4 | ± 4.8 |
| 250 – 350 | 0.32±0.02 | ± 3.4 | ± 5.5 |
| 350 – 800 | 0.018±0.002 | ± 6.2 | ± 11 |

| $m_{t\bar{t}}$ [GeV] | $\frac{1}{\sigma}\frac{d\sigma}{dm_{t\bar{t}}}$ $[10^{-3}\mathrm{GeV}^{-1}]$ | Stat. [%] | Syst. [%] |
|---|---|---|---|
| 250 – 450 | 2.52±0.08 | ± 0.9 | ± 3.1 |
| 450 – 550 | 2.76±0.08 | ± 1.1 | ± 2.8 |
| 550 – 700 | 1.01±0.05 | ± 1.6 | ± 4.2 |
| 700 – 950 | 0.23±0.02 | ± 2.7 | ± 6.3 |
| 950 –2700 | 0.0071±0.0007 | ± 4.2 | ± 8.5 |

| $p_T^{t\bar{t}}$ [GeV] | $\frac{1}{\sigma}\frac{d\sigma}{dp_T^{t\bar{t}}}$ $[10^{-3}\mathrm{GeV}^{-1}]$ | Stat. [%] | Syst. [%] |
|---|---|---|---|
| 0 – 40 | 14.1±0.9 | ± 1.3 | ± 6.2 |
| 40 – 170 | 3.0±0.2 | ± 1.8 | ± 7.4 |
| 170 – 340 | 0.25±0.04 | ± 4.2 | ± 16 |
| 340 –1000 | 0.008±0.001 | ± 7.8 | ± 16 |

| $\lvert y_{t\bar{t}}\rvert$ | $\frac{1}{\sigma}\frac{d\sigma}{d\lvert y_{t\bar{t}}\rvert}$ | Stat. [%] | Syst. [%] |
|---|---|---|---|
| 0.0 – 0.5 | 0.86±0.03 | ± 0.9 | ± 3.2 |
| 0.5 – 1.0 | 0.64±0.01 | ± 0.8 | ± 1.6 |
| 1.0 – 2.5 | 0.17±0.01 | ± 1.8 | ± 7.5 |

# Comparison Data vs MC [1]

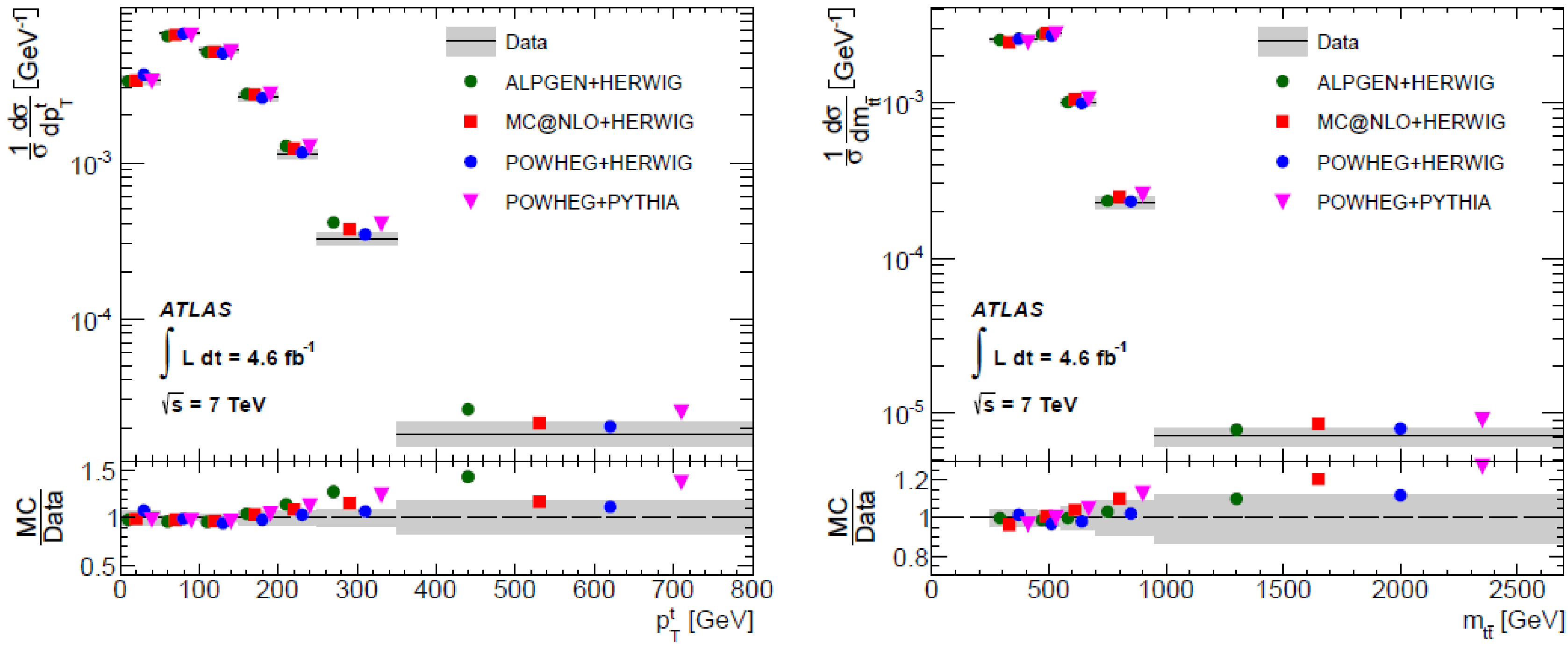


FIG. 8. (Color online) Normalized differential cross-sections for the (a) transverse momentum of the hadronically decaying top quark ($p_{\mathrm{T}}^{t}$), and the (b) mass ($m_{t\bar{t}}$), (c) transverse momentum ($p_{\mathrm{T}}^{t\bar{t}}$) and the (d) absolute value of the rapidity ($|y_{t\bar{t}}|$) of the $t\bar{t}$ system. Generator predictions are shown as markers for ALPGEN+HERWIG (circles), MC@NLO+HERWIG (squares), POWHEG+HERWIG (triangles) and POWHEG+PYTHIA (inverted triangles). The markers are offset within each bin to allow for better visibility. The gray bands indicate the total uncertainty on the data in each bin. The lower part of each figure shows the ratio of the generator predictions to data. For $p_{\mathrm{T}}^{t\bar{t}}$ the POWHEG+PYTHIA marker cannot be seen in the last bin of the ratio plot because it falls beyond the axis range. The cross-section in each bin is given as the integral of the differential cross-section over the bin width, divided by the bin width. The calculation of the cross-sections in the last bins includes events falling outside of the bin edges, and the normalization is done within the quoted bin width. The bin ranges along the horizontal axis (and not the position of the markers) can be associated with the normalized differential cross-section values along the vertical axis.

# Comparison Data vs MC [2]

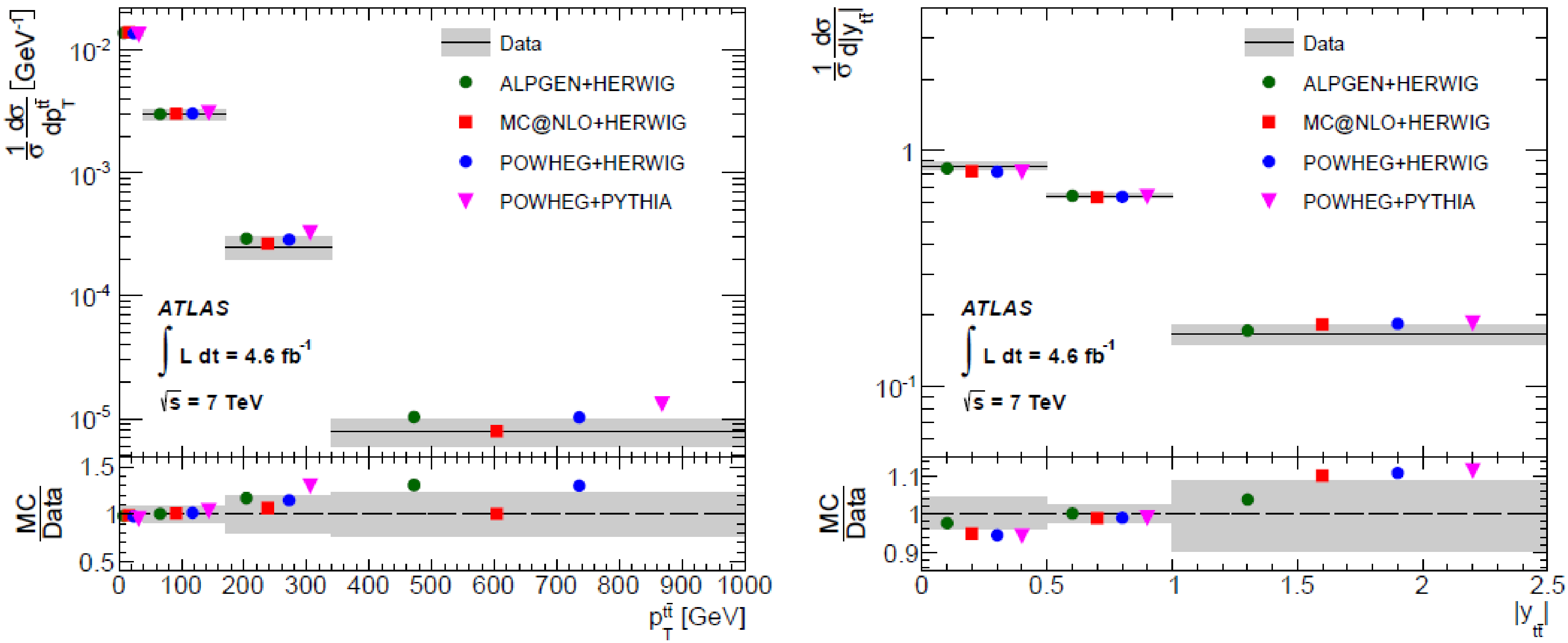


FIG. 8. (Color online) Normalized differential cross-sections for the (a) transverse momentum of the hadronically decaying top quark ($p_T^t$), and the (b) mass ($m_{t\bar{t}}$), (c) transverse momentum ($p_T^{t\bar{t}}$) and the (d) absolute value of the rapidity ($|y_{t\bar{t}}|$) of the $t\bar{t}$ system. Generator predictions are shown as markers for ALPGEN+HERWIG (circles), MC@NLO+HERWIG (squares), POWHEG+HERWIG (triangles) and POWHEG+PYTHIA (inverted triangles). The markers are offset within each bin to allow for better visibility. The gray bands indicate the total uncertainty on the data in each bin. The lower part of each figure shows the ratio of the generator predictions to data. For $p_T^{t\bar{t}}$ the POWHEG+PYTHIA marker cannot be seen in the last bin of the ratio plot because it falls beyond the axis range. The cross-section in each bin is given as the integral of the differential cross-section over the bin width, divided by the bin width. The calculation of the cross-sections in the last bins includes events falling outside of the bin edges, and the normalization is done within the quoted bin width. The bin ranges along the horizontal axis (and not the position of the markers) can be associated with the normalized differential cross-section values along the vertical axis.

# Comparison Data vs MC [3]

- No single generator performs **best** for all the kinematic variables
- ✓ The difference in $\chi^2$ between generators demonstrates that the **data** have sufficient **precision** to probe the predictions.

- For top $p_T$ the agreement with Alpgen+Herwig and Powheg+Pythia is particularly bad due to a significant discrepancy in the tail of the distribution: general trend of data being **softer in $p_T$** above 200 GeV compared to all generators.

| Variable | ALPGEN+HERWIG | | MC@NLO+HERWIG | | POWHEG+HERWIG | | POWHEG+PYTHIA | | NLO QCD | | NLO+NNLL | |
|---|---|---|---|---|---|---|---|---|---|---|---|---|
| | $\chi^2$/NDF | $p$-value | $\chi^2$/NDF | $p$-value | $\chi^2$/NDF | $p$-value | $\chi^2$/NDF | $p$-value | $\chi^2$/NDF | $p$-value | $\chi^2$/NDF | $p$-value |
| $p_T^t$ | 24./6 | 0.00 | 8.0/6 | 0.24 | 4.8/6 | 0.57 | 19./6 | 0.00 | 9.5/6 | 0.15 | 7.6/6 | 0.27 |
| $m_{t\bar{t}}$ | 2.6/4 | 0.63 | 6.9/4 | 0.14 | 5.5/4 | 0.24 | 13./4 | 0.01 | 5.5/4 | 0.24 | 5.9/4 | 0.20 |
| $p_T^{t\bar{t}}$ | 4.2/3 | 0.25 | 0.5/3 | 0.93 | 4.1/3 | 0.26 | 21./3 | 0.00 | 14./3 | 0.00 | 9.9/3 | 0.02 |
| $\lvert y_{t\bar{t}}\rvert$ | 1.6/2 | 0.45 | 3.4/2 | 0.18 | 4.3/2 | 0.11 | 4.8/2 | 0.09 | 3.7/2 | 0.16 | | |

TABLE VII. Comparison between the measured normalized differential cross-sections and the predictions from several MC generators and theoretical calculations. For each variable and prediction a $\chi^2$ and a $p$-value are calculated using the covariance matrix of each measured spectrum. The number of degrees of freedom (NDF) is equal to $N_b - 1$ where $N_b$ is the number of bins in the distribution. In the last column $p_T^t$, $m_{t\bar{t}}$ and $p_T^{t\bar{t}}$ are compared to NLO+NNLL predictions [11] and [12–14].

# Dependance on PDFs choice

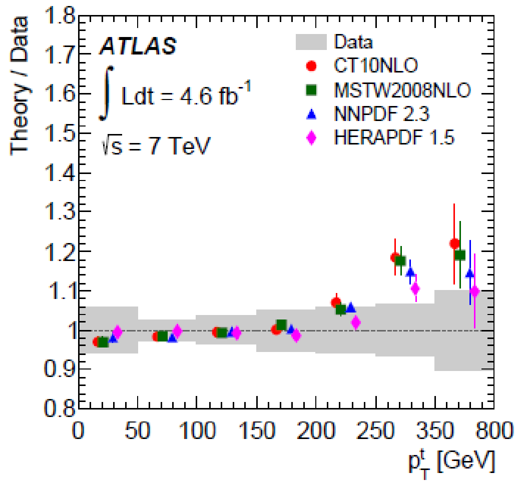


(a)

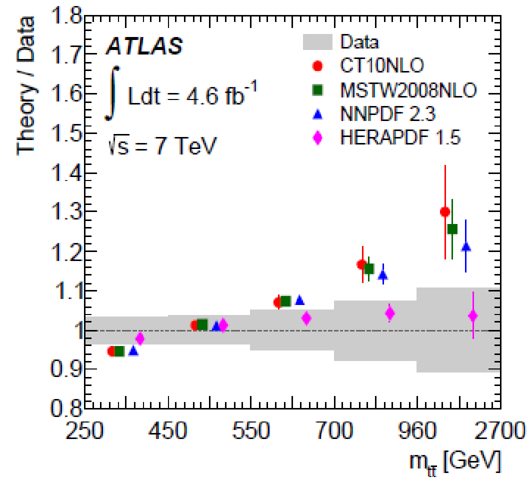


(b)

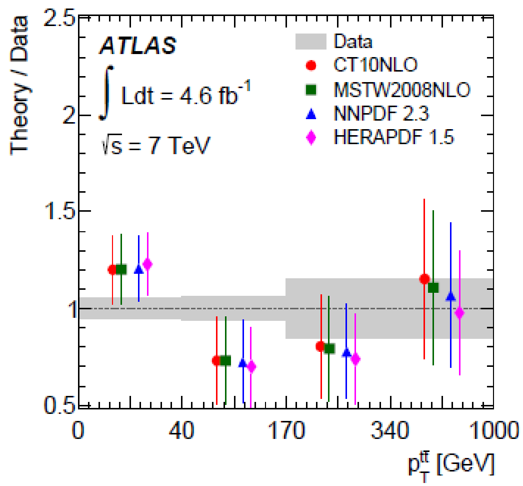


(c)

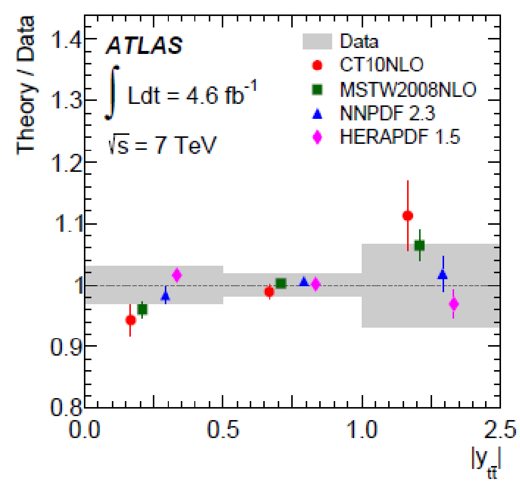


(d)

Some preference for HERAPDF when used with a fixed order NLO QCD calculation

# Comparison Data vs Theory

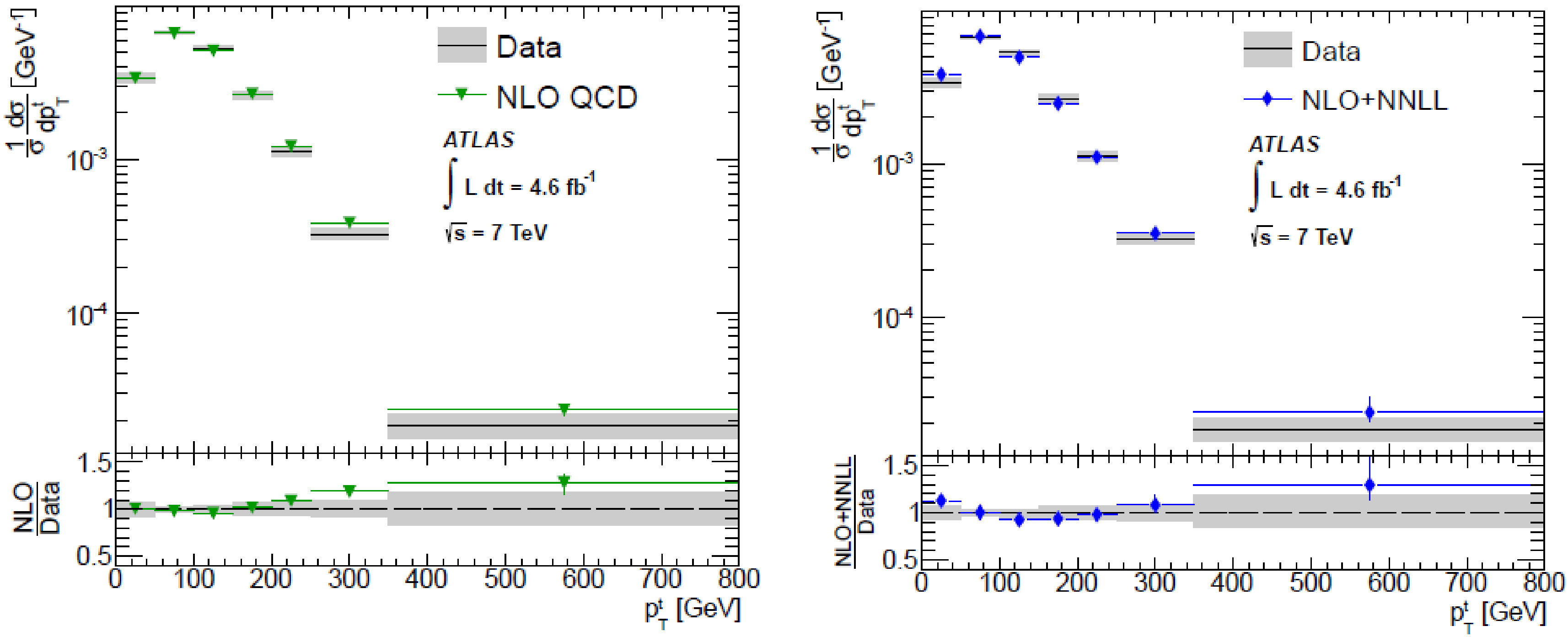


- ✓ Overall agreement
- ➢ In the high $p_T$ region the data tends to be below the prediction.

# Summary

- The **measurement of normalized differential cross section** for ttbar production has been performed by the ATLAS experiment in the lepton+jets decay channel.

- The **dataset** corresponds to 4.6 $fb^{-1}$ integrated luminosity at a center of mass energy of 7 TeV.

✓ The **integrated cross section** agrees with the SM prediction.

✓ The **differential cross section** as a function of different kinematic variables has been measured and it fairly agrees with the predictions.

✓ The precision of the measurement allows to **discriminate** between different MC generators and parton distribution functions.

➢ However, no MC generator performs better for **all** kinematic variables, while the distributions show some preference for the HERAPDF 1.5.

# Thanks for your attention